APROKSIMATIVNI IZRAZI GREEN-OVE FUNKCIJE POLNESKONČNEGA ELASTIČNEGA MEDIJA

TOMAŽ PLIBERŠEK IN ANDREJ UMEK

o avtorjih

Tomaž Pliberšek
Univerza v Mariboru,
Fakulteta za gradbeništvo
Smetanova 17, 2000 Maribor, Slovenija
E-pošta: tomaz.plibersek@uni-mb.si

Andrej Umek
Univerza v Mariboru,
Fakulteta za gradbeništvo
Smetanova 17, 2000 Maribor, Slovenija
E-pošta: umek@uni-mb.si

izvleček

Greenova funkcija homogenega in slojevitega pol-prostora na površini obremenjenega s harmonično, koncentrirano silo poljubne smeri je v splošnem podana z integralno predstavitvijo. Izvrednotenje te predstavitve v diskretnih točkah je matematično zahtevno in zahteva veliko računalniškega časa. Avtorja sta v svojih predhodnih člankih izvrednotenje Greenove funkcije poenostavila tako, da sta iz pol-neskončnega Hankelovega integrala izdvojila singularni del, del ki je vezan na površinske valove in preostali del pretvorila v integral preko končnega integracijskega območja, ki je manj zahteven za izvrednotenje. Inženirska praksa preračuna dinamičnih lastnosti in neintruzivne identifikacije temeljnih tal nakazujeta potrebo po nadaljnji poenostavitvi izrazov za Greenovo funkcijo.

Članek obravnava razvoj aproksimativnih funkcij za določevanje pomikov v tolerancah inženirske natančnosti na osnovi eksaktno diskretiziranih komponent Greenove funkcije. Njihova natančnost bi naj bila boljša kot so tolerance intruzivnih merskih podatkov identifikacije mehanskih karakteristik zemljine. Verjamemo, da bo uporaba v članku izpeljanih aproksimativnih izrazov zmanjšala matematični napor pri reševanju interakcijskih problemov konstrukcija - zemljina istočasno pa odprla nove možnosti za neintruzivne identifikacije zemljin.

ključne besede

elasto-dinamika, pol-prostor, Greenova funkcija, aproksimativne rešitve

APPROXIMATE EXPRESSIONS FOR THE GREEN'S FUNCTIONS OF A SEMI-INFINITE, ELASTIC MEDIUM

TOMAŽ PLIBERŠEK and ANDREJ UMEK

About the authors

Tomaž Pliberšek
University of Maribor,
Faculty of Civil Engineering
Smetanova 17, 2000 Maribor, Slovenia
E-mail: tomaz.plibersek@uni-mb.si

Andrej Umek
University of Maribor,
Faculty of Civil Engineering
Smetanova 17, 2000 Maribor, Slovenia
E-mail: umek@uni-mb.si

Abstract

On the basis of an exact, discretized presentation of the Green's function components, their closed-form approximations are developed. Their accuracy is considered to be better than the tolerances in the intrusive measurements data for the identification of the mechanical characteristics of soils. The use of these approximate expressions is believed to considerably reduce the computational effort in soil-structure interaction problems and open up new possibilities for the non-intrusive identification of soils.

Keywords

elastodynamics, half-space, Green's function, approximate solutions

1 INTRODUCTION

The Green's function of a semi-infinite medium yields the best description of the dynamic properties of soil in many problems in soil-structure interaction, earthquake engineering and seismology. Many authors have dealt with the problem of how to determine the Green's function for a semi-infinite elastic medium and have limited their attention to homogeneous and layered half-spaces. The latter appear to be the most general case of structured half-spaces for which an analytical expression can be derived. We further limit our attention to the surface displacements Green's function due to a unit, harmonic point force. It has been shown that these displacements can be expressed through semi-infinite integrals, e.g., Lamb [1], Ewing et al. [2], Wolf [3] etc., of the form:

$$u_{i,j}(a) = \int_0^\infty f_{i,j}(\eta) \cdot J_n(a \cdot \eta) d\eta \qquad (1)$$

where $u_{i,j}$ is one of the displacement components and i describes its coordinate direction. In the most commonly used cylindrical coordinate system, therefore, i stands for r, ϑ and z, respectively. j describes the direction of the unit, harmonic force acting on the surface of the semi-infinite medium. $f_{i,j}$ is the characteristic function of the problem. Its poles and branch cuts are associated with the surface and body waves of the particular problem, respectively. J_n is a Bessel function of the first kind and nth order. In the treated problem n can take the values 0, 1 and 2. And, finally, a is the dimensionless distance from the source point given by:

$$a = \frac{r \cdot \omega}{v_s} \qquad (2)$$

where r is the physical distance from the source point, ω is the angular velocity of the harmonic excitation and v_s is the shear wave velocity in the uppermost layer of the layered half-space and in the homogeneous half-space, respectively.

The integrals (1) cannot be evaluated analytically, not even in the simplest case of a homogeneous half-space. Their numerical evaluation is highly demanding and time-consuming for two reasons. We have, due to the presence of the Bessel function J_n, to cope with an oscillating integrand and for the components of the Green's function, which are singular at its origin, the portions of the integration paths near and at infinity contribute significantly to the value of the integrals. Furthermore, the latter ones determine the type of the singularity at the point of the origin of the Green's function. Many authors have explored the possibilities of how to perform the numerical integration. Their attempts ran

in two different directions. The first group, e.g., Kobori et al. [4], Stade and Layton [5], Zhielkin and Kukarkin [6], Lemoin [7], Secada [8], Lucas and Stone [9], Wang et al. [10], Martinez-Castro and Gallego [11], etc., kept the original integration path along the positive real axis of the integration variable from 0 to ∞ and used a special integration algorithm known as the Fast Fourier-Bessel transform (FFBT). The procedure proposed by the above-mentioned authors differs slightly from one to the other, but they have several factors in common. With the use of the FFBT algorithm they avoided the problems with an oscillating integrand. However, some of the problems remained, which can be clearly seen from the basic concept of this algorithm. Its principal idea is to introduce the integral representation of the Bessel function J_n into the Eq. (1) and then exchange the orders of the integration. This yields the following:

$$u_i(a) = \frac{i^n}{2\pi} \int_{-\pi}^{\pi} e^{in\alpha}\, d\alpha \int_0^{\infty} f_{i,j}(\eta) e^{-ia\eta\cos\alpha}\, d\eta \qquad (3)$$

The inner integral can be viewed as a Fourier transform of the function $f_{i,j}$ in the transform variable $a\cos\alpha$, if we consider it as:

$$f_{i,j}(\eta) = \begin{cases} f_{i,j}(\eta), & \eta \geq 0 \\ 0, & \eta < 0 \end{cases} \qquad (4)$$

Therefore, the inner integral of Eq. (3) can be, in principle, efficiently numerically evaluated by a Fast Fourier Transform (FFT) algorithm, leading to an easy numerical integration over a finite range. However, using the FFBT algorithm we are still faced with two significant problems. A more detailed analysis of the functions $f_{i,j}$ shows that for the components of the Green's function, which are singular at the origin, gilts:

$$\lim_{\eta\to\infty} f_{i,j}(\eta) \neq 0 \qquad (5)$$

Therefore, the conditions for the existence of the Fourier Transform, as e.g., given by Sneddon [12], are not satisfied and therefore the Fast Fourier Transform (FFT) of this part of the integrand is of questionable validity, as noted by Pliberšek and Umek [13]. Some of the authors were apparently aware of this fact, e.g., Vostroukhov et al. [14]. They avoided this problem by replacing the point force through a statically equivalent loading distributed over a small area and obtained by the Saint-Venant principle the Green's function with satisfying accuracy except at, and close to, its origin. The others split the Green's function components into their regular and singular parts, respectively. The right-hand side of equation (1) thus becomes:

$$u_i(a) = \frac{\lim\limits_{\eta\to\infty} f_{i,j}(\eta)}{a} \left(1 + \frac{a}{\lim\limits_{\eta\to\infty} f_{i,j}(\eta)} \int_0^{\infty} g_{i,j}(\eta) J_n(a\eta)\, d\eta \right) \qquad (6)$$

where $g_{i,j}$ is defined as:

$$g_{i,j}(\eta) = f_{i,j}(\eta) - \lim_{\eta\to\infty} f_{i,j}(\eta) \qquad (7)$$

The extraction of singularity ensured that the Fourier transform of the function $g_{i,j}$ exists; however, the other apparent difficulty that we integrate in the case of no material damping through its singularities and in the case of some material damping, which is usually the realistic case, close to its singularities remains. From Eq. (7) it is clear that the singularities of the function $f_{i,j}$ are also present in the function $g_{i,j}$ since they differ by a constant only. In the case of zero material damping in at least one of the layers one should add to the Fourier integral the contributions coming from small semicircles around the poles of the integrand. In the case of small material damping, conducting the integration path close to the poles of the integrand can lead to numerical instabilities, as reported by Kobori et al. [4].

The first attempts known to us to avoid the described problems and to transform the integral in Eq. (6) to a new integration path are those of Kobayashi and Sassaki [15] and Kobayashi [16]. They limited their attention to a homogeneous half-space and succeeded in transforming the semi-infinite integrals to keyhole integrals along a suitably chosen branch cut, which they further reduced to the integral from zero to one. The latter one has to be evaluated numerically, however, without any numerical difficulties and instabilities. Štrukelj et al. [17] and Pliberšek et al. [18] and [19] extended Kobayashi's approach to the case of layered media. They reduced the semi-infinite inversion integrals to a number of keyhole integrals, where their number is equal to the number of layers in the case that internal damping within the layers is different.

Whichever of the above-described approaches we chose, the results obtained are in the form of discrete values of the Green's function components at chosen dimensionless distances from the source point. Such a presentation is suitable to be used e.g., in soil-structure interaction problems, although it requires more computational effort than the closed-form solution in the case that the latter could be obtained. The discretized data solution is, however, not suitable for a number of technically relevant tasks. It cannot be used for a direct identification of the Green's function from non-intrusive measurements; it also can not be used for the soil identification via the

Green's function, which would parallel the better-known SASW method. With all this in mind we present in this paper approximate, closed-form expressions for the Green's function components. The bounds for the error were set in such a way that the differences between the exact, discretized presentation and the presented approximate expressions are not larger than the tolerances during the intrusive measurements data. In this paper we limit our attention to the homogeneous half-spaces.

2 BASIC CONCEPT OF THE APPROXIMATION

The approximation to the Green's function for a semi-infinite medium can derived on the basis of Eq. (1) and (6), respectively. We decided to proceed from Eq. (6). This starting point has two advantages. The first one is that all the integrals appearing in this equation, regardless of the Green's function component considered, show the same basic behavior and are expressed in the same general form. This is, however, not the case with the integrals in equation (1), where some of them exhibit singular behavior at the source point and the others do not. Therefore, the method developed to approximate one of the integrals in Eq. (6) can be applied to the others. The only difference between the components that, are singular at the origin and those that are not, is that for the latter ones the constant is equal to zero and for the former ones it is a well-determined value. However, all the integrals:

$$\lim_{\eta \to \infty} f_{i,j}(\eta) \qquad (8)$$

Regardless of whether they belong to the components of the Green's function, which are singular or regular at the source point, behave in the same way. The second advantage of this approach is that the singular term in the Green's function, where it exists, is given exactly. In many important practical applications, e.g., soil-structure interaction problems, only the values of the Green's function over small distances from the source point are required and there the singular term is the dominant one. Therefore, extracting the singularity greatly improves the accuracy of the approximation.

From the literature, e.g., [20] and [21], several asymptotic expansions of the integrals are known. It can be, however, concluded that the integral in Eq. (6) and given by Eq. (8) cannot be transformed to any one of the standard examples. The Bessel function in the integrand prevents us from transforming it to a Laplace-type integral:

$$I_{i,j}(a) = \int_0^\infty g_{i,j}(\eta) J_n(a\eta) d\eta \qquad (9)$$

as given by Miklowitz [20], on which the method of steepest descent is based, nor to a Fourier-type integral:

$$I_L(x) = \int_a^b f(t) e^{x g(t)} dt \qquad (10)$$

which is the foundation for the stationary phase method. The third possibility, also presented by Miklowitz [20], would be the integration per-parts approach. It is from the structure of the integral, defined by Eq. (10), clear that this approach also does not lead to a desired asymptotic expansion of the Green's function. The first one or two steps show that we have to deal with the derivatives of the Bessel function, which make the expressions obtained too complicated and no clear convergence could be established.

After realizing that in wave mechanics standard approximations of integrals do not yield satisfactory results, we are left with two options. The first one would be to approximate the integrands in Eq. (6) by a suitably chosen family of functions in the sense of the L_2 norm and then conduct the integration. The second one is to approximate the integral in the same sense.

To decide on which of these two types of approximation of the integral in Eq. (6) is more appropriate, we first need to study the behavior of its integrand. It is clear that the integrand is the product of two functions, which behave extremely differently. The function $g_{i,j}(\eta)$ is a relatively slow varying function except in the vicinity of its poles and branch points, which lie in the case of zero material damping on the integration path and, in the case of realistically assumed material damping, close to it. The second function, the Bessel function, is a smooth but oscillating function. The characteristic behavior of these functions for zero and 0.03 material damping is presented in Fig. 1 and 3. The characteristic behavior of the integrand as a whole is given in Fig 2 and 4.

The combination of the oscillatory behavior of the Bessel function with the rapid changes of the function $g_{i,j}$, close to their singularities and their smooth behavior far from them, represent a considerable difficulty in approximating the integrand through one or a combination of the families of the functions most commonly used in numerical mathematics, i.e., polynomials and exponential functions of the real and imaginary argument, respectively [22]. Therefore, the integrand in Eq. (6) cannot be considered as an appropriate starting point to derive the approximation.

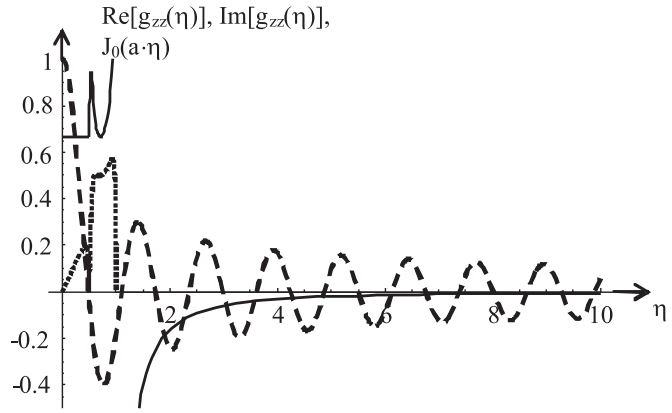

Figure 1. Parts of the integrand for the vertical displacements due to a unit vertical force: real part of the function $g_{zz}(\eta)$, the solid line; imaginary part of the function $g_{zz}(\eta)$, the dotted line; and the Bessel function $J_0(a\cdot\eta)$, the broken line. The following values for the material constants have been assumed: Poisson's ratio $\nu=\frac{1}{3}$, material damping h=0 and the dimensionless distance a=5.

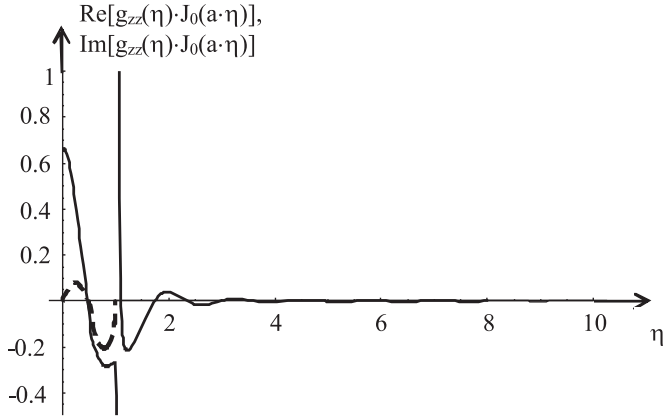

Figure 2. The integrand for the vertical displacements due to a unit vertical force: the real part is given by the solid and the imaginary part by the broken line. The following values for material have been assumed: Poisson's ratio $\nu=\frac{1}{3}$, material damping h=0 and the dimensionless distance a=5.

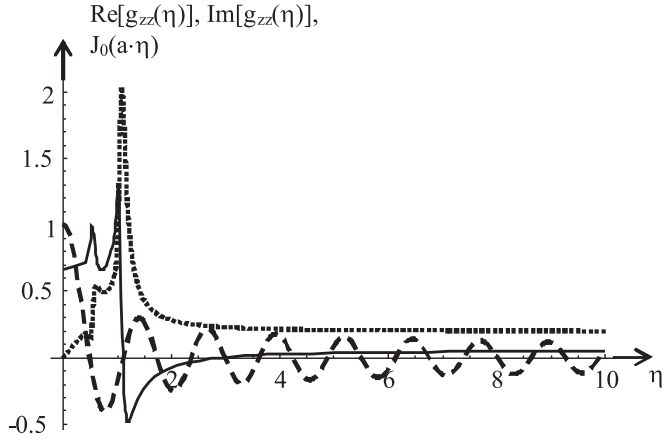

Figure 3. Parts of the integrand for the vertical displacements due to a unit vertical force: real part of the function $g_{zz}(\eta)$, the solid line; imaginary part of the function $g_{zz}(\eta)$, the dotted line; and the Bessel function $J_0(a\cdot\eta)$, the broken line. The following values for the material constants have been assumed: Poisson's ratio $\nu=\frac{1}{3}$, material damping h=0.03 and the dimensionless distance a=5.

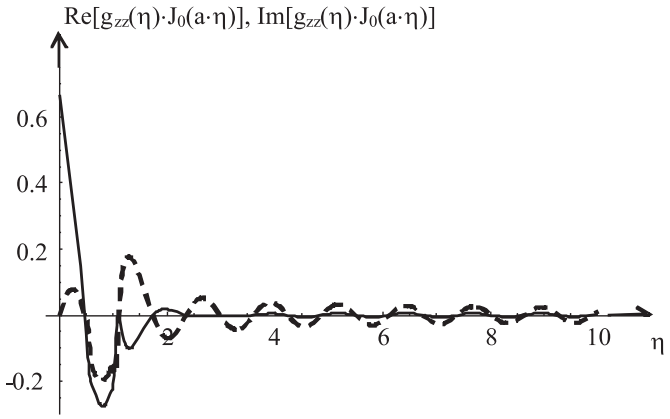

Figure 4. The integrand for the vertical displacements due to a unit vertical force: the real part is given by the solid and the imaginary part by the broken line. The following values for the material constants have been assumed: Poisson's ratio $\nu = \frac{1}{3}$, material damping h=0.03 and the dimensionless distance a=5.

We now turn our attention to the integral in Eq. (6), which is given by Eq. (8). In the example presented in Figure 5 we can see that the integration smoothes the rapid and irregular changes of the integrand. The result is a function that, is characterized by a fairly regular oscillation with a smooth and decreasing envelope, and these observations apply to the real as well as to the imaginary part of the integral. Therefore, the integrals $I_{i,j}(a)$ are chosen as a basis for the approximation. It is also clear that the polynomials are not the best family of functions to approximate curves, like those presented in Figure 5. Therefore, we chose as a basis for the approximation a combination of trigonometric and exponential functions of the real argument. Some promising combinations are examined in detail in the next paragraph.

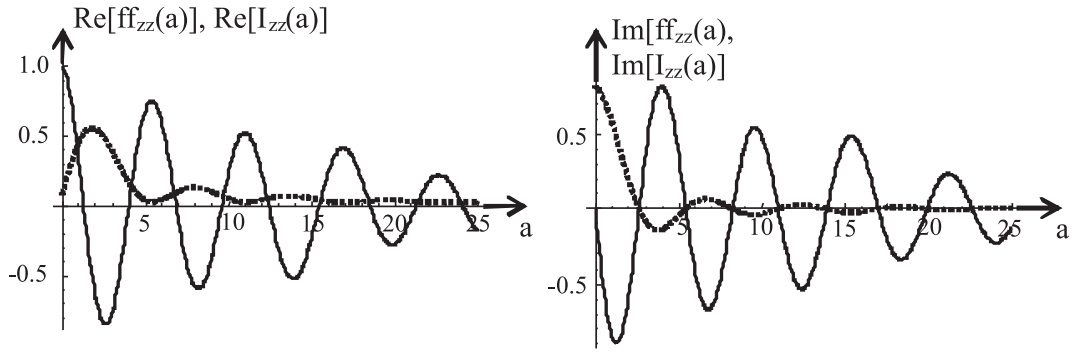

Figure 5. Comparison of the integral $I_{zz}(a)$ with the corresponding fundamental function.

From Figure 5 it can also be seen that the fundamental function, which is defined as:

$$ff_{i,j}(a) = 1 + \frac{a}{\lim\limits_{\eta\to\infty} f_{i,j}(\eta)} \int_0^\infty g_{i,j}(\eta) J_n(a\,\eta) d\eta \qquad (11)$$

is a more suitable choice for the approximation, once we have decided to use the trigonometric and exponential functions of the real argument as families of the approximating functions.

On the basis of Figures 5 and 6 (next page) and other components studied, the following approximation was investigated in detail:

$$\left.\begin{matrix}\mathrm{Re}\\ \mathrm{Im}\end{matrix}\right\}(ff_{i,j}(a)) \approx \left.\begin{matrix}\mathrm{Re}\\ \mathrm{Im}\end{matrix}\right\}(apff_{i,j}(a)) = \sum_{i=1}^{n} e^{-\gamma_i a} \cdot c_i \cdot \left.\begin{matrix}\sin\\ \cos\end{matrix}\right\}(b_i \cdot a) \qquad (12)$$

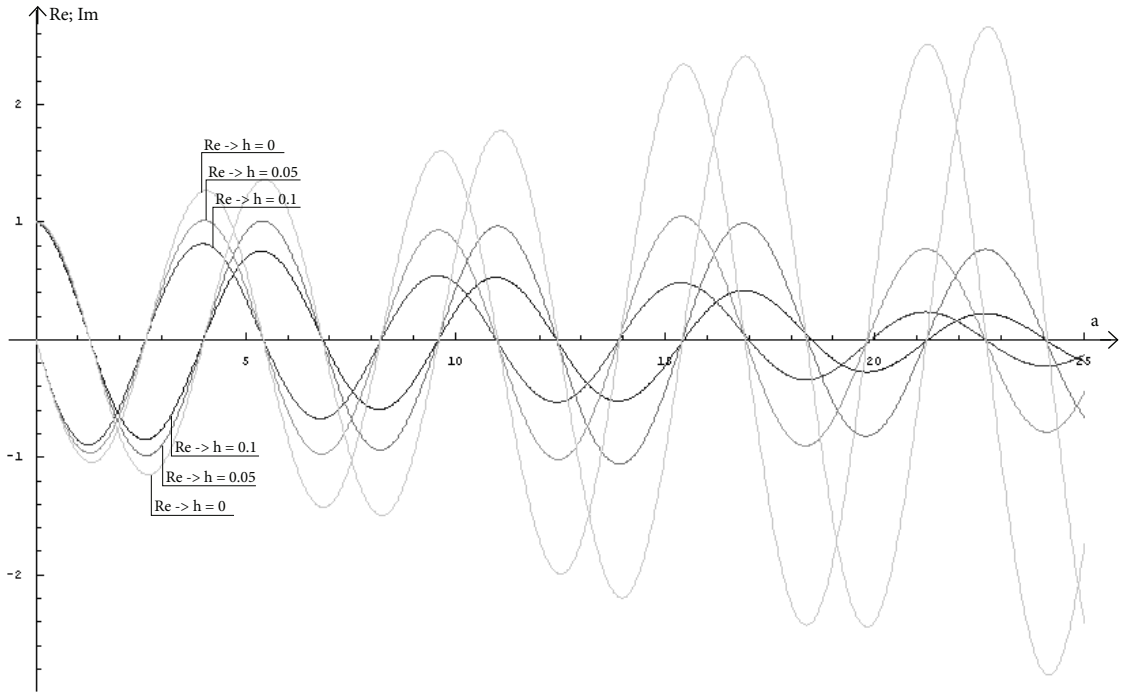

Figure 6. The fundamental function for the vertical displacement due to a unit vertical force for the chosen material damping values. The Poisson's ratio $\nu = \frac{1}{3}$ has been assumed.

The real and imaginary parts of the fundamental functions were approximated independently from each other, as indicated by the symbol $\left.\begin{matrix}\mathrm{Re}\\ \mathrm{Im}\end{matrix}\right\}$. In their approximations the sinuses or cosinuses were applied, indicated by the symbol $\left.\begin{matrix}\sin\\ \cos\end{matrix}\right\}$, the former ones in the case that the value of the fundamental function at a=0 is zero and the cosinuses otherwise. For the approximate fundamental function the symbol $ap_{ffi,j}(a)$ is used.

3 ILLUSTRATIVE EXAMPLE

For the illustrative example, the fundamental function for the vertical displacement due to the vertical unit, the harmonic force has been chosen and the range of the dimensionless distance a, given by Eq. (2), from 0 to 25 has been selected. It is believed that this range of dimensionless distance is sufficient for the problems of soil-structure interaction and Green's function identification. Two different material dampings were considered, h=0.10 and h=0.03. The first one stands for the soils with relatively high damping and the second for the soils with low damping. The number of terms in the approximation was chosen to be one, two and three, respectively. The best-fit approximations were performed using the program Matematica.

3.1 ONE-TERM APPROXIMATION

In the on-term approximation we use:

$$\mathrm{Re}(ff_{z,z}(a)) \approx \mathrm{Re}(apff_{z,z}(a)) = c_1 \cdot e^{-\gamma_1 \cdot a} \cdot \cos(b_1 \cdot a) \qquad (13)$$

and

$$\mathrm{Im}(ff_{z,z}(a)) \approx \mathrm{Im}(apff_{z,z}(a)) = c_2 \cdot e^{-\gamma_2 \cdot a} \cdot \sin(b_2 \cdot a) \qquad (14)$$

The least-squares approximation for the internal damping h=0.10 yields the following values for the coefficients in equations (13) and (14):

c_1=0.995985	γ_1=0.0596105	b_1=1.12597
c_2=-0.985963	γ_2=0.0581773	b_2=1.12614

The comparison between the exact results following Kobayshi's approach and the approximation derived above is shown in Fig. 7.

The error in the above-defined approximation is:

$$err_1 = \frac{1}{25.0} \cdot \int_0^{25.0} \left[\mathrm{Re}(ff_{z,z}(a)) - \mathrm{Re}(apff_{z,z}(a))\right]^2 da = 0.00669295 \qquad (15)$$

and

$$err_2 = \frac{1}{25.0} \cdot \int_0^{25.0} \left[\mathrm{Im}(ff_{z,z}(a)) - \mathrm{Im}(apff_{z,z}(a))\right]^2 da = 0.00667756 \qquad (16)$$

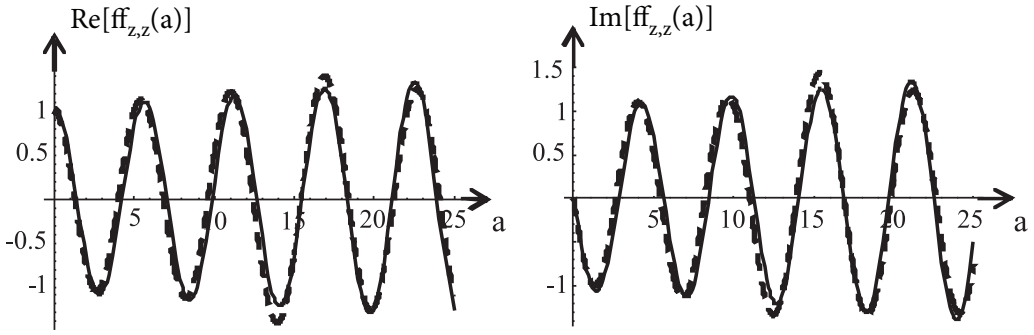

Figure 7. Comparison of the exact fundamental function $f_{zz}(a)$, given by the broken line; and its one-term approximation, given by the solid line. The material damping was assumed to be h=0.10.

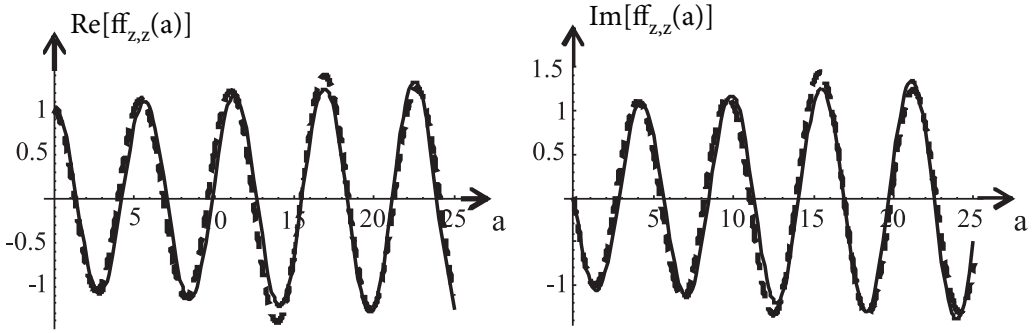

Figure 8. Comparison of the exact fundamental function $f_{zz}(a)$, given by the broken line; and its one-term approximation, given by the solid line. The material damping was assumed to be h=0.03.

For the material damping h=0.03 the least-squares approximation yields:

c_1=1.0507	γ_1=-0.0106777	b_1=1.11609
c_2=-1.03608	γ_2=-0.0122008	b_2=1.11682

The comparison between the exact and appreciative values of the fundamental function is shown in Figure 8. The material damping was assumed to be h=0.03. The error for this case is:

For the real part the approximation is:

$$err_3 = \frac{1}{25.0}\cdot\int_0^{25.0}\left[\mathrm{Re}(ff_{z,z}(a)) - \mathrm{Re}(apff_{z,z}(a))\right]^2 da = 0.0325395 \quad (17)$$

and for the imaginary part, respectively:

$$err_4 = \frac{1}{25.0}\cdot\int_0^{25.0}\left[\mathrm{Im}(ff_{z,z}(a)) - \mathrm{Im}(apff_{z,z}(a))\right]^2 da = 0.0312312 \quad (18)$$

3.2 TWO-TERMS APPROXIMATION

In the two-terms approximation we use:

$$\mathrm{Re}(ff_{z,z}(a)) \approx \mathrm{Re}(apff_{z,z}(a)) = \sum_{i=1}^{2} c_i \cdot e^{-\gamma_i \cdot a} \cdot \cos(b_i \cdot a) \quad (19)$$

and

$$\mathrm{Im}(ff_{z,z}(a)) \approx \mathrm{Im}(apff_{z,z}(a)) = \sum_{i=1}^{2} c_{i+2} \cdot e^{-\gamma_{i+2} \cdot a} \cdot \sin(b_{i+2} \cdot a) \quad (20)$$

Following the same procedure as in the one-term approximation the coefficients in equations (19) and (20) for the material damping h=0.10 are determined. They are as follows:

c_1=-1.5	γ_1=0.120606	b_1=1.01333
c_2=2.50383	γ_2=0.109332	b_2=1.08702
c_3=-0.259736	γ_3=-0.0143126	b_3=1.08191
c_4=-0.692457	γ_4=0.0637071	b_4=1.18805

On the basis of the above-listed coefficients, the errors were computed. They are, for the real part:

$$err_1 = \frac{1}{25.0} \cdot \int_0^{25.0} \left[\mathrm{Re}(ff_{z,z}(a)) - \mathrm{Re}(apff_{z,z}(a)) \right]^2 da = 0.00123647 \quad (21)$$

and for the imaginary part:

$$err_2 = \frac{1}{25.0} \cdot \int_0^{25.0} \left[\mathrm{Im}(ff_{z,z}(a)) - \mathrm{Im}(apff_{z,z}(a)) \right]^2 da = 0.00238762 \quad (22)$$

respectively. For the material damping h=0.03 the following values were obtained:

c_1=-0.552778	γ_1=0.0307106	b_1=0.968259
c_2=1.54378	γ_2=0.0197715	b_2=1.10899
c_3=-1.85541	γ_3=0.0272306	b_3=1.10019
c_4=0.849891	γ_4=0.0394818	b_4=0.99098

The corresponding errors are:

$$err_3 = \frac{1}{25.0} \cdot \int_0^{25.0} \left[\mathrm{Re}(ff_{z,z}(a)) - \mathrm{Re}(apff_{z,z}(a)) \right]^2 da = 0.00347543 \quad (23)$$

and

$$err_4 = \frac{1}{25.0} \cdot \int_0^{25.0} \left[\mathrm{Im}(ff_{z,z}(a)) - \mathrm{Im}(apff_{z,z}(a)) \right]^2 da = 0.00348752 \quad (24)$$

3.3 THREE-TERMS APPROXIMATION

In the three-terms approximation we use:

$$\mathrm{Re}(ff_{z,z}(a)) \approx \mathrm{Re}(apff_{z,z}(a)) = \sum_{i=1}^{3} c_i \cdot e^{-\gamma_i \cdot a} \cdot \cos(b_i \cdot a) \quad (25)$$

and

$$\mathrm{Im}(ff_{z,z}(a)) \approx \mathrm{Im}(apff_{z,z}(a)) = \sum_{i=1}^{3} c_{i+3} \cdot e^{-\gamma_{i+3} \cdot a} \cdot \sin(b_{i+3} \cdot a) \quad (26)$$

The coefficients in equations (25) and (26) for the half-space with material damping h=0.10 are:

c_1=0.640348	γ_1=0.0259827	b_1=1.11881
c_2=0.37689	γ_2=0.111726	b_2=1.25876
c_3=-0.0230052	γ_3=-0.0752526	b_3=0.861735
c_4=-1.53327	γ_4=0.100735	b_4=1.10478
c_5=0.476431	γ_5=0.076713	b_5=0.954981
c_6=0.0601061	γ_6=0.013543	b_6=0.493489

The corresponding errors are:

$$err_1 = \frac{1}{25.0} \cdot \int_0^{25.0} \left[\mathrm{Re}(ff_{z,z}(a)) - \mathrm{Re}(apff_{z,z}(a)) \right]^2 da = 0.000894818 \quad (27)$$

for the real and

$$err_2 = \frac{1}{25.0} \cdot \int_0^{25.0} \left[\mathrm{Im}(ff_{z,z}(a)) - \mathrm{Im}(apff_{z,z}(a)) \right]^2 da = 0.0000275089 \quad (28)$$

for the imaginary part, respectively. We now turn our attention to the three-terms approximation for the case when the material damping is 0.03. The following coefficients were computed for this case:

c_1=0.726239	γ_1=0.0269564	b_1=1.18327
c_2=0.336632	γ_2=-0.068329	b_2=1.10594
c_3=-0.0492427	γ_3=-0.0950448	b_3=0.868245
c_4=-0.530666	γ_4=-0.0570736	b_4=1.10957
c_5=-0.455507	γ_5=0.0101311	b_5=1.22544
c_6=0.0352293	γ_6=-0.106017	b_6=0.856865

The errors for this case are:

$$err_3 = \frac{1}{25.0} \cdot \int_0^{25.0} \left[\mathrm{Re}(ff_{z,z}(a)) - \mathrm{Re}(apff_{z,z}(a)) \right]^2 da = 0.00202942 \quad (29)$$

and

$$err_4 = \frac{1}{25.0} \cdot \int_0^{25.0} \left[\mathrm{Im}(ff_{z,z}(a)) - \mathrm{Im}(apff_{z,z}(a)) \right]^2 da = 0.00249281 \quad (30)$$

4 DISCUSSION OF THE RESULTS AND CONCLUSIONS

The error analysis for all three cases the one-, two- and three-term approximations of the fundamental function and for both representative material dampings clearly show that the components of the Green's function for the homogeneous half space can be, in the framework of engineering accuracy, approximated by a simple, closed-form analytical expression. These closed-form analytical expressions can be used, on the one hand, to significantly reduce the numerical effort in soil-structure interaction problems and, on the other hand, to identify the mechanical properties of the soil through non-intrusive methods by measuring the induced vibration of the half space and identifying the coefficients in equation (12).

From the error estimates presented in the preceding paragraph it can be concluded that the one-term approximation is accurate enough for most engineering purposes. Adding additional terms to the one-term expression leads to the two- and three-term formulas and reduces the errors. The significant reduction of the

error is limited to the transition from the one- to two-term formulas. The subsequent error reduction are less pronounced, and therefore we stopped our analysis after three terms. On the other hand, the numerical effort in deriving three- and more-term formulas increases significantly and also leads to the formulas of higher complexity with no, from the engineering view point, significant gains in accuracy. It is believed that one- and two-term formulas are the most useful. The choice of the former or the latter depends on the problem they will be used.

It is clear that higher material damping permits a better approximation than with the lower one. This is due to the fact that the exponential envelope we used in our work, which can be seen from equation (12), is more suitable for higher material damping. Despite the fact that relevant engineering approximations of the Green's function components were obtained, we believe that in the definition of the most suitable mathematical formulation of the envelope there is still some room for improvements.

REFERENCES

[1] A[1] Lamb, H. (1904). On the Propagation of Tremors over the Surface of an Elastic Solid. Phil. Trans. A 203, 1 – 42.

[2] Ewing, M.W., Jardetzky, W.S., Press, F. (1957). Elastic waves in layered media. McGraw-Hill Book Company, New York.

[3] Wolf, J.P., 1985. Dynamic Soil – Structure Interaction. Prentice – Hall, Inc., Englewood Cliffs, New Jersey.

[4] Kobori, T., Miura, K., Moroi, T. (1987). Fast Fourier Bessel Transform for Calculating the Green's Function for Semi-Infinite Soil Media. 3rd Int. Conf. Soil Dyn. Earthq. Eng. Vol. 3, 365-374.

[5] Stade, E., Layton, E.G. (1995). Generalized discrete Fourier transforms: the discrete Fourier-Riccati-Bessel transform. Computer Physics Communications 85, 336-370.

[6] Zhielkin, Ya.M., Kukarkin, A.B. (1995). On an algorithm for the fast Fourier-Bessel transform (in Russian). Zh. Vychisl. Mat. i Mat. Fiz. 35 (7), 1128-1133.

[7] Lemoin, D. (1997). Optimal cylindrical and spherical Bessel transforms satisfying bound state boundary conditions. Computer Physics Communications 99, 297-306.

[8] Secada, J.D. (1999). Numerical evaluation of the Hankel transform. Computer Physics Communications 116, 278-294.

[9] Lucas, S.K., Stone, H.A. (1995). Evaluating infinite integrals involving Bessel functions of arbitrary order. Journal of Computational and Applied Mathematics 64, 217-231.

[10] Wang, C.D., Tzeng, C.S., Pan, E., Liao, J.J. (2003). Displacements and Stresses due to a vertical point load in an inhomogeneous transversely isotropic half-space. International Journal of Rock Mechanics and Mining Sciences 40, 667-685.

[11] Martinez-Castro, A.E., Gallego, R. (2007). Three-dimensional Green's function for time-harmonic dynamics in a viscoelastic layer. International Journal of Solids and Structures (IJSS) 44, 4541-4558.

[12] Sneddon, I.H. (1972), The use of integral transforms, McGraw-Hill, New York.

[13] Pliberšek, T., Umek, A. On the evaluation of the Green's function of semi-infinite, layered elastic medium. International Journal of Solids and Structures (IJSS), under review.

[14] Vostroukhov, A.V., Verichev, S.N., Kok, A.W.M. and Esveld, C. (2004). Steady-state response of stratified half-space subjected to a horizontal arbitrary buried uniform load applied at a circular area. Soil Dynamics and Earthquake Engineering 24, 449-459.

[15] Kobayashi, T., Sasaki, F. (1991). Evaluation of Green's function on semi-infinite elastic medium. KICT Report No.86, Kajima Technical Research Institute, Kajima Corporation.

[16] Kobayashi, T. (1981). Evaluation of response to point load excitation on semi-infinite elastic medium (in Japanese). Tran. Archi. Institute., Japan 302, 29-35.

[17] Štrukelj, A., Pliberšek, T., Umek, A. (2006). Evaluation of Green's function for vertical point load excitation applied to the surface of a layered semi-infinite elastic medium. Arch. Appl. Mech. (AAM) 76, 465-479.

[18] Pliberšek, T., Štrukelj, A., Umek, A. (2005). Green's function for an elastic layer loaded harmonically on its surface. Acta Geotechnica Slovenica (AGS) 2 (1), 4-21.

[19] Pliberšek T., Umek A. (2008). Green's function for tangentially loaded layered half-space. Acta Geotechnica Slovenica (AGS), 5 (1), 50-69.

[20] Miklowitz, J. (1978). The Theory of Elastic Waves and Waveguides, North-Holland. Amsterdam, pp. 250 – 297.

[21] Erdelyi, A. (1956). Asymptotic expansions. Dover, New York.

[22] Hamming, R.W.(1973). Numerical methods for scientist and Engineers. McGraw-Hill, New York.